ACS APPLIED MATERIALS & INTERFACES

Research Article

www.acsami.org

Localized Surface Plasmon Resonance Detection of Biological Toxins Using Cell Surface Oligosaccharides on Glyco Chips

Takehiro Nagatsuka,[†] Hirotaka Uzawa,*[,†] Keita Sato,[†] Satoshi Kondo,[†] Masayuki Izumi,[†] Kenji Yokoyama,[†] Isaac Ohsawa,[‡] Yasuo Seto,[‡] Paola Neri,[§] Hiroshi Mori,[§] Yoshihiro Nishida,[⊥] Masato Saito,[∥] and Eiichi Tamiya[∥]

[†]Nanosystem Research Institute, National Institute of Advanced Industrial Science and Technology (AIST), 1-1-1 Higashi, Tsukuba 305-8565, Japan

[‡]National Research Institute of Police Science, 6-3-1 Kashiwanoha, Kashiwa, Chiba 277-0882, Japan

[§]Department of Biopharmaceutical Sciences, Gifu Pharmaceutical University, 1-25-4, Daigaku-nishi, Gifu 501-1196, Japan

[⊥]Nano-biology, Graduate School of Advanced Integration Science, Chiba University, Matsudo 271-8510, Japan

[∥]Department of Applied Physics, Graduate School of Engineering, Osaka University, 2-1 Yamadaoka, Suita, Osaka 565-0871, Japan

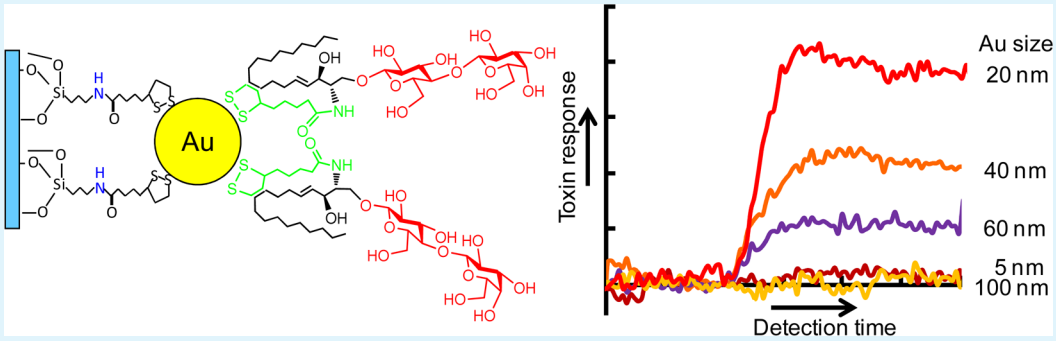

ABSTRACT: We have detected biological toxins using localized surface plasmon resonance (LSPR) and synthetic glycosyl ceramides (β-lactoside, globosyl trisaccharide (Gb_3), or GM1 pentasaccharide) attached to gold (Au) nanoparticles. The particle diameters ranged from 5−100 nm. The detection sensitivity for three toxins (ricin, Shiga toxin, and cholera toxin) was found to depend not only on the attached glycoside but also on the diameter of the Au nanoparticles. For the detection of ricin, the 20-nm β-lactoside-coated Au nanoparticle exhibited the highest LSPR response, whereas 40-nm Gb_3- and GM1-coated Au nanoparticles gave the best results for Shiga toxin and cholera toxin, respectively. In addition, a blocking process on the nanoparticle surface greatly improved the detection sensitivity for cholera toxin. The LSPR system enabled us to detect ricin at 30 ng/mL, Shiga toxin at 10 ng/mL, and the cholera toxin at 20 ng/mL.

KEYWORDS: *localized surface plasmon resonance, biological toxin, detection, carbohydrate, gold nanoparticle, sensitivity*

INTRODUCTION

Localized surface plasmon resonance (LSPR) is a new and powerful technique for analyzing intermolecular interactions of biomacromolecules.[1,2] It is being applied to the analysis of antigen−antibody reactions,[3,4] as well as for the clinical diagnosis of microbial infections[5] and Alzheimer's diseases.[6] Generally for these analyses, proteins[7−10] or polynucleotides (DNA or RNA)[11,12] are immobilized on nanoparticles, nanorods, or nanoprisms to make LSPR biochips. LSPR chips coated with smaller biomolecules are also being investigated; for example, D-mannose was used for the LSPR analysis of lectins and *Escherichia coli*.[13,14] Since carbohydrate molecules, especially host cell−surface oligosaccharides, are known to bind microbes and biological toxins,[15] such "glyco-chips" could be used with LSPR to allow detection of microbes and toxins.

Previously, we detected biological toxins with synthetic oligosaccharides together with surface plasmon resonance (SPR) and quartz crystal microbalance (QCM) analyses.[16−18] When compared with SPR and QCM, LSPR may have some advantages in terms of cost performance and field transportation, the latter being highly advantageous for on-site detection of biological toxins. In the present study, our goal was to develop a portable LSPR detection system that uses glyco-chips containing Au nanoparticles coated with synthetic oligosaccharides that specifically bind toxins.

In the present study, ricin, Shiga toxin, and cholera toxin were selected as the toxin targets. Since ricin from *Ricinus communis* has been used in bioterrorism,[19] counter-measures are urgently required. Shiga toxin produced from *E. coli* O157 is a highly toxic protein that is categorized as a scheduled

Received: January 22, 2013
Accepted: April 29, 2013
Published: May 13, 2013

   dx.doi.org/10.1021/am4002937 | *ACS Appl. Mater. Interfaces* 2013, 5, 4173−4180

compound in the Chemical Weapon Convention and is also ranked as category B by the Centers for Disease Control and Prevention (USA).[20] The toxin often causes hemolytic uremic syndrome and other systemic complications.[21] Cholera toxin from *Vibrio cholerae* may be less toxic than the other two; however, it has caused food poisoning worldwide.[22] All of these toxins recognize host cell−surface oligosaccharides and enter into the host cell by way of endocytosis. We effectively apply these natural recognition events in our LSPR system.

EXPERIMENTAL SECTION

Materials and Instruments. Ricin from *Ricinus communis* was obtained from the Honen Corporation (Tokyo, Japan) and was safely handled at the National Research Institute of Police Science with approval of the Minister of Economy, Trade and Industry of Japan (http://www.meti.go.jp/polycy/chemical_management/cwc/200kokunai/202horitu_gaiyo.htm). Cholera toxin was purchased from WAKO Chemicals (Osaka, Japan). Shiga toxin was obtained as reported previously.[17,18] Peanut (*Arachis hypogaea*) and wheat germ (*Triticum vulgaris*) lectins were supplied from WAKO Chemicals. Lectins from *Sambucus nigra* and horse gram (*Dolichos biflorus*) were purchased from EY Laboratories (San Mateo, CA, USA). Bovine serum albumin (BSA) was obtained from Kokusan-kagaku (Tokyo, Japan). Lactoside (**1**) was synthesized as reported previously.[16] Ganglioside GM1 was purchased from WAKO Chemicals. Sphingolipid ceramide *N*-deacylase (SCDase, E.C. 3.5.1.69) was obtained from TAKARA Bioscience (Shiga, Japan). *lyso*-Ceramide trihexoside (*lyso*-Gb_3) was supplied by Matreya LLC (Pleasant Gap, PA, USA). Au nanoparticles were supplied from Sigma-Aldrich (5 and 20 nm, St. Louis, MO, USA), from Tanaka Precious Metals (40 nm, Tokyo, Japan), and from SPI Supplies/Structure Probe, Inc. (60 and 100 nm, West Chester, PA, USA). Reaction monitoring and electrospray ionization mass spectra (ESI-MS) were carried out using a SHIMADZU LC-MS 2010A mass spectrometer (Kyoto, Japan). Microwave-irradiated sugar immobilization was carried out using a Wave Magic MWO-1000S (2.45 GHz, Tokyo Rikakikai Co. Ltd., Tokyo, Japan). A tungsten halogen light source (LS-1), 400-μm core diameter optical fibers (P400-1-UV/vis), and a spectrometer (QE65000, bandwidth: 475−851 nm) with a long-path filter (OF1-GG475) were purchased from Ocean Optics (Dunedin, FL, USA). A flowing pump (TE-361N) was obtained from Terumo (Tokyo, Japan). A Peltier-controlled cuvette holder (qpod) with Z-height of 15 mm was purchased from Quantum Northwest (Liberty Lake, WA, USA). A sample injector (Rheodyne 9725 or 7725) was obtained from IDEX Health & Science LLC (Rohnert Park, WA, USA). A flow cell (FLAB50-UV-02) was obtained from GL Science (Tokyo, Japan). All other reagents were commercially available.

Synthesis of 2. A solution of *lyso*-ceramide trihexoside (*lyso*-Gb_3) (5.7 mg) and *N*-hydroxysuccinimidyl (NHS) ester of lipoic acid (3.3 mg) in dry DMF (1 mL) was stirred at rt for 24 h. The mixture was then purified by reverse-phase HPLC with a column of X-Bridge (10 mm i.d. × 25 cm, Waters, Milford, MS, USA) eluted with methanol at a flow rate of 3 mL/min to afford **2** (4.3 mg, total yield: 60%). $[\alpha]_D$ +21 (*c* 0.17, MeOH). ^{1}H NMR (600 MHz, CD_3OD): δ 5.683 (ddd, 1H, —CH═C*H*—CH_2—, *J* = 6.8 Hz, 15.4 Hz), 5.446 (dd, 1H, —*CH*═CH—CH_2—, *J* = 7.7 Hz, 15.4 Hz), 4.941 (d, 1H, Gal H-1′, *J* = 3.6 Hz), 4.401 (d, 1H, Gal H-1, *J* = 7.3 Hz), 4.302 (dd, 1H, Glc H-1, *J* = 7.7 and 0.72 Hz), 4.248 (br t, 1H, *J* = 6.6 Hz), 4.148 (m, 1H), 4.066 (br t, 1H, *J* = 8.1 Hz), 3.861 (dd, 1H, H-6, *J* = 4.4 and 12.2 Hz), 3.809 (dd, 1H, *J* = 3.7 and 10.3 Hz), 3.764 (dd, 1H, *J* = 3.3 and 10.3 Hz), 3.728 (dd, 1H, *J* = 7.7 and 11.4 Hz), 3.195−3.150 (m, 1H, —CH_2—CH_2—S—), 3.198−3.070 (m, 1H, —CH_2—CH_2—S—), 2.50−2.44 (m, 1H, —CH_2—CH_2—S—), 2.25−2.15 (m, 2H, —C(O)—CH_2—CH_2—), 2.05−2.00 (br, 2H, —CH═CH—CH_2—CH_2—), 1.92−1.85 (m, 1H, —CH_2—CH_2—S—), 1.75−1.57, 1.50−1.40 (2 × m, 6H, *N*-thioctyl), 1.40−1.25 (m, —(CH_2)—), 0.892 (t, 3H, —CH_2—CH_3, *J* = 7.1 Hz). ESI-MS (positive) calcd for $C_{44}H_{79}NO_{18}S_2Na$: $[M + Na]^+$ 996.5. Found: 996.5. ESI-MS (negative) calcd for $C_{45}H_{80}NO_{20}S_2$: $[M + HCOO]^+$ 1018.5. Found: 1018.7.

Synthesis of 3. Ganglioside GM1 (10 mg) containing an almost equimolar mixture of C_{18} and C_{20} sphingosine isomers was dissolved in a 100 mM AcONa−AcOH buffer (pH 5.8, 1.0 mL), followed by the addition of 2.6 mL of water and 8 mg/mL of taurodeoxycholate (0.4 mL). A total of 50 μL of sphingolipid ceramide *N*-deacylase (SCDase, 5 mU/μL) was added, and the reaction mixture was covered with 20 mL of *n*-decane and incubated at 37 °C for 2 weeks. Aliquots were periodically analyzed by HPLC-MS. When the reaction was nearly complete, the mixture was frozen at −20 °C and the *n*-decane was removed. The thawed mixture was applied to a column (4.6 mm i.d. × 25 cm) packed with X-Bridge C_{18} resin (Waters). The column was eluted with 60% aqueous methanol to remove taurodeoxycholate and then 80% aqueous methanol to yield the *lyso*-GM1. **C_{18**-*lyso*-**GM1** (3.85 mg, 47%) calcd: $[M + H]^+$ 1280.62. Found: positive $[M + H]^+$ 1280.35, negative $[M - H]^-$ 1278.50. **C_{20**-*lyso*-**GM1** (2.07 mg, 25%) calcd: $[M + H]^+$ 1308.65. Found: positive $[M + H]^+$ 1308.30, negative $[M]^-$ 1307.65.

A solution of C_{18}-*lyso*-GM1 (6.6 mg) and NHS ester of lipoic acid (4.7 mg) in dry DMF (0.64 mL) was stirred at rt for 21 h following the same procedure as described for compound **2** to give **3** (3.85 mg, 50%). Calcd: $[M]^+$ 1467.65. Found: negative $[M + H]^+$ 1468.60. $[\alpha]_D$ −0.88 (*c* 0.15, MeOH).

Preparation of Sugar-Modified LSPR Chips. Glass plates were cleaned with piranha solution (H_2O_2/H_2SO_4 = 1/3, v/v) at 80 °C for 40 min and treated with 10% 3-aminopropyltrimethoxysilane in ethanol for 15 min. (*Caution*: piranha solution reacts violently with organic materials and should be handled with extreme care.) The glass plates were rinsed with ethanol and dried at 50 °C for 3 h under vacuum. After cooling, the plates were treated with 16.5 mM NHS ester of lipoic acid in DMF (20 mL) at rt for 48 h under N_2 atmosphere. The lipoic acid modified plates were then treated with Au nanoparticles (5 nm, 20 nm, 40 nm, 60 nm, and 100 nm) for 6 h to give the LSPR chips.

Lactoside **1** was immobilized on the LSPR chip using self-assembly. The LSPR chip was placed in lactoside **1** in methanol (50 μg/mL, 2 mL), and the sugar immobilization was performed under 250-W microwave irradiation at 45 °C for 60 min. After cooling, the lactose-modified LSPR chip was extensively washed with methanol and water. Gb_3 trisaccharide **2** and GM1 pentasaccharide **3** were similarly immobilized on LSPR chips. The GM1-modified LSPR chip was further blocked with lipoic acid in methanol (5 mM) for 1−2 min, followed by rinsing with methanol and water.

Detection of Toxins with LSPR. The LSPR system consists of a tungsten halogen light source, a portable flow pump, an injection valve with a sample loop for 250 μL or 1 mL, a flow cell (0.025 mm optical length) that can be disassembled for attachment of the prepared LSPR chips, a temperature-controlled sample compartment with a Peltier-controlled cuvette holder, a spectrometer for detection of absorbance changes, and a PC for data analysis. The flowing buffer was 10 mM HEPES (pH 7.5) containing 150 mM NaCl, filtered with a 0.22 μm filter and degassed before use. The buffer was run in the LSPR system until the baseline was stable. A total of 250 μL of ricin at concentrations of 30 ng/mL or 100 ng/mL were injected into the LSPR system for 7.5 min at a flow rate of 33.3 μL/min. Similarly, 1 mL of the cholera toxin (20 ng/mL, 50 ng/mL, or 100 ng/mL) or Shiga toxin (10 ng/mL or 100 ng/mL) was injected for 15 min at a flow rate of 66.6 μL/min. Concentrations of lectins from peanut (*Arachis hypogaea*), wheat germ (*Triticum vulgaris*), *Sambucus nigra*, horse gram (*Dolichos biflorus*), and BSA were 300 ng/mL. The detection temperature was 25 °C, the integration time was 8 ms, and 2000 accumulations were acquired for each data set. In general, a LSPR system detects a wavelength shift when analytes bind to or dissociate from the sensor chip surface. In the present study, a change of absorbance at a fixed wavelength was detected instead. The absorbance at 550 nm (A_{550}) was used as the response signal for detection. The absorbance at 720 nm (A_{720}) was used as a reference because it is not affected by toxin binding. All LSPR data were analyzed with OOIBase32 software (Ocean Optics, version 2.0).

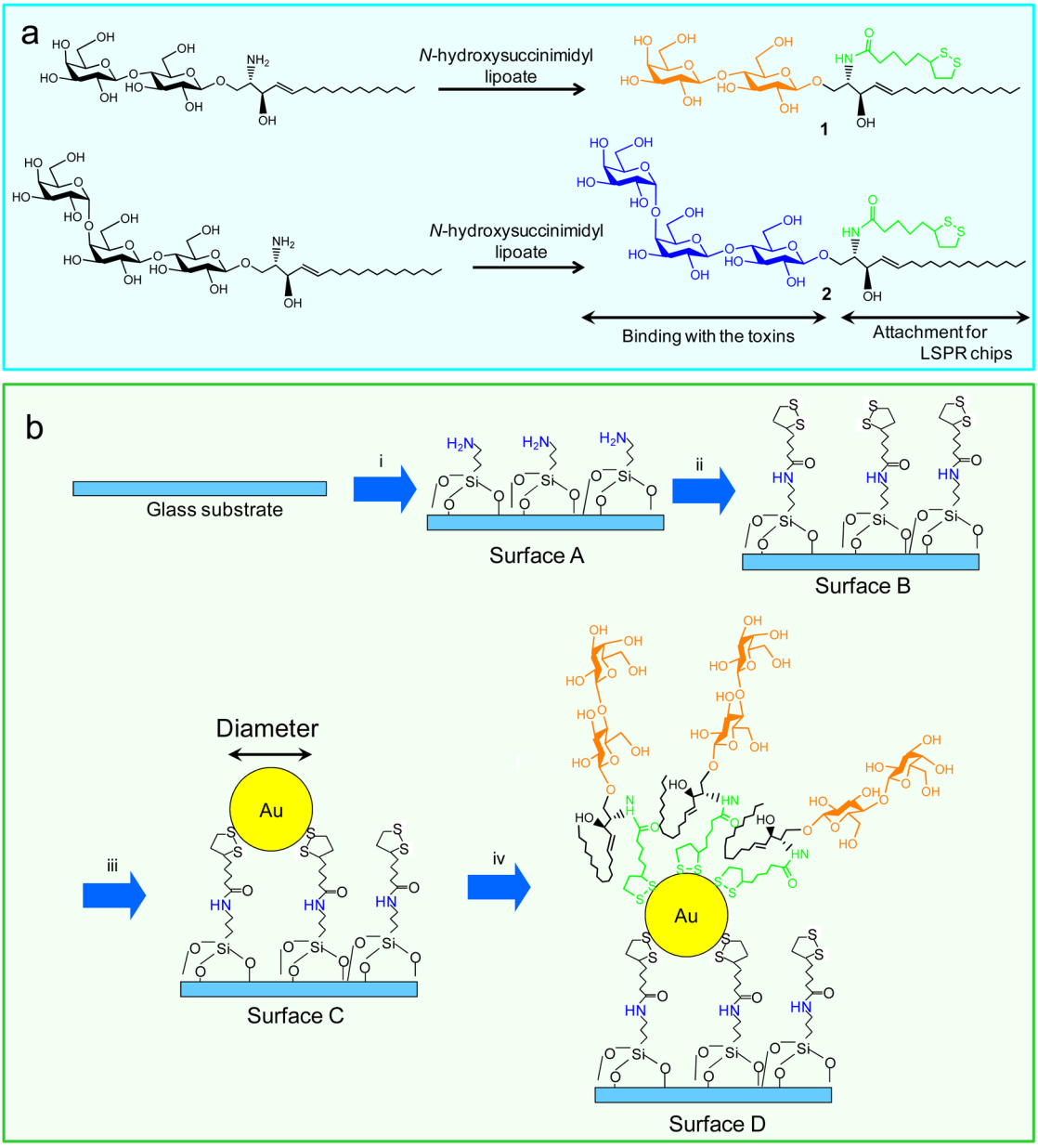

Figure 1. (a) Synthesis of lactoside **1** and Gb_3 trisaccharide **2**, carrying lipoic acids in the aglycons. (b) Preparation of LSPR chips. Reaction conditions: (i) 3-aminopropyltrimethoxysilane, then heated at 50 °C for 3 h under vacuum, (ii) *N*-hydroxysuccinimidyl (NHS) ester of lipoic acid, (iii) Au nanoparticles (diameters: 5, 20, 40, 60, and 100 nm), and (iv) 50 μg/mL of lactoside **1** in methanol under microwave irradiation (45 °C, 60 min). The Gb_3-chip was derived using **2** in the same way as the lactosyl chip.

Safety Considerations. Ricin, cholera toxin, and Shiga toxin are highly toxic if inhaled or digested. These toxins should be handled with special care. After use, they must be destroyed (denatured) with sodium hypochlorite or an autoclave.

RESULTS AND DISCUSION

LSPR Glyco-Chips Functionalized with β-Lactoside (Lac) and Globotriaoside (Gb_3) for the Detection of Ricin and Shiga Toxins (Stx). Ricin binds to β-D-galactopyranosyl or *N*-acetyl-β-D-galactosaminyl residues on host cells.[23−27] Shiga toxins recognize globotriaosyl (Gb_3) ceramides expressed on human cells, where they cluster in "rafts" or microdomains.[28−31] Therefore, we applied β-lactosyl ceramide (**1**) and Gb_3 ceramide (**2**) as depicted in Figure 1a. These compounds carry a lipoic acid in aglycon and thus can be immobilized on Au nanoparticles via self-assembly. They were prepared from the *lyso*-compounds using *N*-hydroxysuccinimidyl (NHS) ester of lipoic acid as shown in Figure 1a.[16]

LSPR chips were prepared as shown in Figure 1b. Clean glass substrates were treated with 3-aminopropyltrimethoxysilane and heated at 50 °C for 3 h under reduced pressure to produce glass surface A having terminal amino groups. NHS ester of lipoic acid was reacted with the amino group on surface A by a conventional chemical pathway to produce surface B having disulfide (S−S) bonds. Au nanoparticles with various diameters (5, 20, 40, 60, and 100 nm) were deposited on surface B to obtain surface C. In these processes, Au nanoparticles were immobilized on surface B via self-assembly in a manner similar to that reported previously.[16] The resulting surface C was treated with each of the carbohydrate ligands **1** and **2** to yield surface D. In all cases, there was no evidence of aggregated Au

dx.doi.org/10.1021/am4002937 | ACS Appl. Mater. Interfaces 2013, 5, 4173−4180

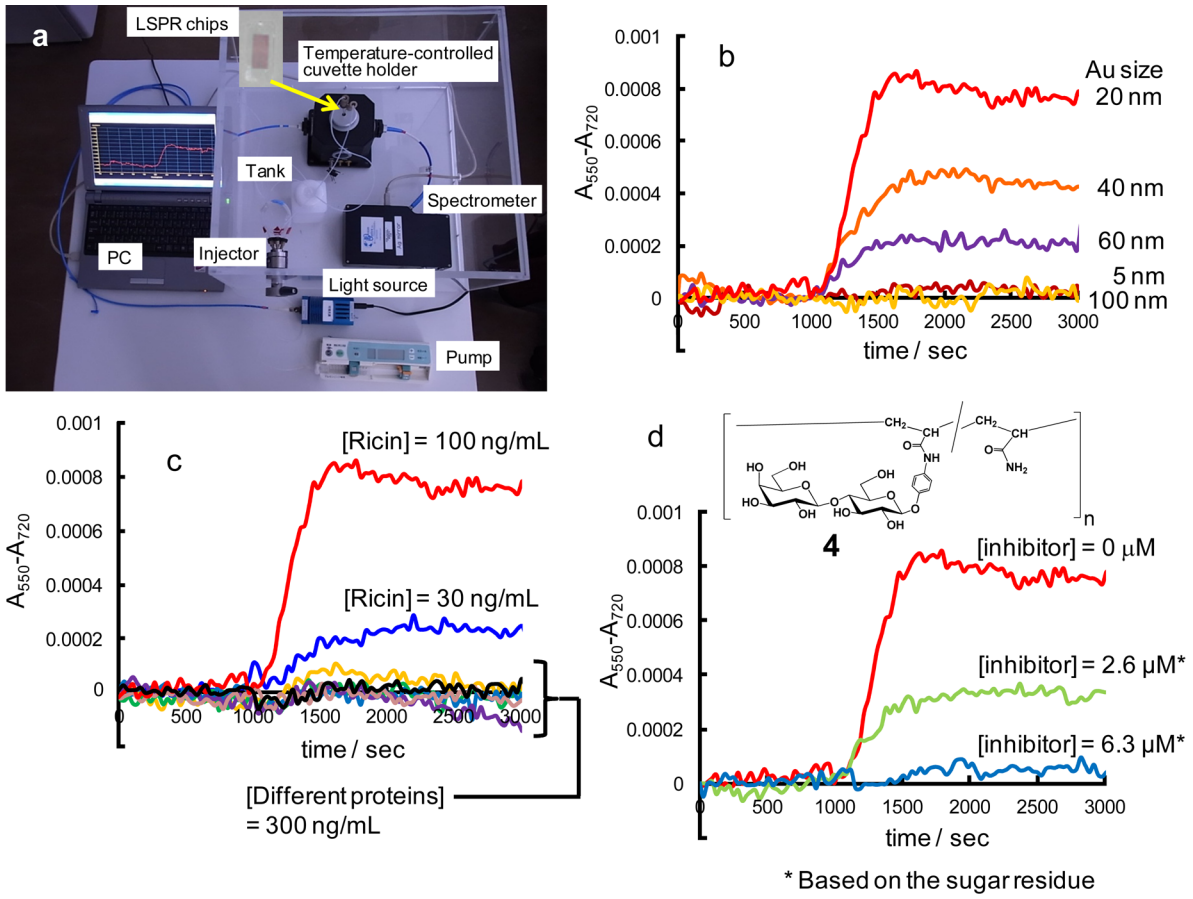

Figure 2. LSPR detection of ricin using lactose-functionalized chips: (a) Photo of LSPR system. (b) Effect of Au nanoparticle diameter on the detection of ricin (100 ng/mL). (c) Sensitivity and specificity of the lactose chips for 20 nm Au nanoparticles. Other proteins: peanut lectin (300 ng/mL), *Triticum vulgaris* lectin from wheat germ (300 ng/mL), *Sambucus nigra* (300 ng/mL), *Dolichos biflorus* lectin from horse gram (300 ng/mL), BSA (300 ng/mL), and cholera toxin (100 ng/mL). (d) Inhibition assay using glycopolymer **4** as the inhibitor. Au nanoparticle size: 20 nm. [ricin] = 1.68 nM (100 ng/mL). Ricin and glycopolymer **4** were mixed at 25 °C for 60 min. Molar concentrations of the inhibitor are given in panel (d). All samples were injected at 1000 s.

nanoparticles since there was no absorbance at longer wavelengths (>600 nm), and there were no visible blue spots on the surfaces.

The LSPR system is shown in Figure 2a. The optical system has a tungsten halogen light source, a temperature-controlled cuvette holder, and a spectrometer, all connected with optical fibers. The flow system has a portable pump, a flow cell with the sugar-modified LSPR chips, and a tank for wastes. This system is operated with a PC and OOIBase32 software (ver. 2.0).

LSPR Detection of Ricin Using Lactose-Functionalized Chips. For LSPR, Au nanoparticles with established surface geometries, shapes, and sizes should be used. Au nanoparticles with 10−100 nm diameter sizes are widely utilized,[1,3,4,11] while studies on optimal sizes have been reported theoretically[32,33] and experimentally.[34−37] The potential utility of Au nanorods, Au nanostars, Au bipyramids, and other shapes have also been suggested.[1,6−10,12] Here, we tested commercially available spherical Au nanoparticles with various diameters (5, 20, 40, 60, and 100 nm) for the ricin detection system using lactose on the glyco-chip. The results summarized in Figure 2b show that the lactose chips using 5- and 100-nm Au nanoparticles showed poor LSPR responses relative to those chips having Au nanoparticles with intermediate sizes. The chip using 20-nm Au nanoparticles exhibited the highest response, where ricin could be detected at a concentration of 30 ng/mL (panel C).

Figure 2c indicates a linear relationship between the LSPR response and ricin concentration (see also Figure 6). In panel c, BSA, a wheat germ lectin from *Triticum vulgaris* (β-D-GlcNAc specific), a horse gram lectin from *Dolichos biflorus* (α-D-GalNAc specific), and cholera toxin (GM1 specific) were examined as negative controls. A peanut lectin from *Arachis hypogaea* (β-D-Gal specific) and *Sambucus nigra* lectin (β-D-Gal and GalNAc specific) were also used for their selectivity. The lactose chips showed no response to these proteins even at 300 ng/mL concentrations [except for cholera toxin (100 ng/mL)]. Thus the ricin−lactose interaction was very specific, as is observed when ricin recognizes lactose on host cells.

We carried out inhibitory experiments to confirm whether the LSPR responses are based on a specific lactose−toxin interaction. The polyacrylamide-based lactose copolymer[38] (**4**, M_W = 2.2 × 10^5, Lac/acrylamide = 18:82) was used as a competitor. In the presence of glycopolymer **4**, the LSPR responses were increasingly suppressed as the concentration of the inhibitor increased (Figure 2d). At a concentration of 6.3 μM, based on the sugar residue of inhibitor **4**, binding to the LSPR chip was completely inhibited for 1.68 nM ricin. The results indicate that the LSPR responses arise from a specific binding interaction between ricin and lactose.

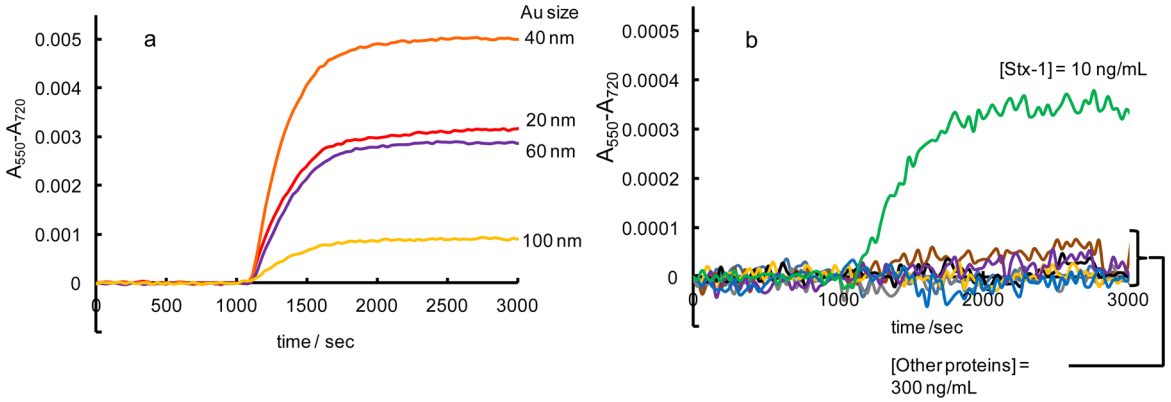

Figure 3. LSPR detection of Stx-1 using the Gb_3 chips. (a) LSPR responses as a function of Au nanoparticle size (20−100 nm) on the Gb_3-chips. [Stx-1] = 100 ng/mL. (b) Detection of Stx-1 and the specificity of the LSPR system using the Gb_3-chips. Au nanoparticle size: 40 nm. Other proteins (300 ng/mL): peanut lectin, *Triticum vulgaris* lectin from wheat germ, *Sambucus nigra*, *Dolichos biflorus* lectin from horse gram, BSA, cholera toxin, and *Ricinus communis* agglutinin (RCA_{120}). All samples were injected at 1000 s.

LSPR Detection of Shiga Toxin Using Gb_3-Functionalized Chips. Gb_3 chips were prepared from Gb_3 trisaccharide **2** that was produced by the reaction of *lyso*-Gb_3 ceramide and NHS ester of lipoic acid (Figure 1) in a similar way to that discussed above for the lactose chips.

Figure 3a shows the effects of Au nanoparticle size (20, 40, 60, and 100 nm) on LSPR responses to Shiga toxin 1 (Stx-1, 100 ng/mL). For Stx-1, Gb_3-chips with 40-nm Au nanoparticles exhibited the highest sensitivity (Figure 3a), which differs from the 20-nm optimum size found for ricin.

Figure 3b shows the results of variable proteins including lectins from peanut (*Arachis hypogaea*), wheat germ (*Triticum vulgaris*), *Sambucus nigra*, horse gram (*Dolichos biflorus*), and *Ricinus communis* agglutinin (RCA_{120}). BSA and cholera toxin were also included. None of these proteins were detected for levels up to 300 ng/mL, indicating that the LSPR system using Gb_3-chips can detect Stx-1 selectively. With this method, we could detect this toxin at 10 ng/mL within 20 min (Figure 3b).

LSPR Detection of Cholera Toxin Using GM1-Functionalized Chips. Cholera toxin (CTX) produced by *Vibrio cholerae* consists of a single A-subunit and pentameric B-subunits.[39,40] The A-subunit activates adenylate cyclases, resulting in constitutive cyclic AMP production. The B-subunits have domains which bind to GM1 gangliosides on the host cell surface. In a manner similar to lactoside (**1**) and Gb_3 trisaccharide (**2**) described in the preceding sections, we designed GM1 pentasaccharide **3** carrying lipoic acid in the aglycon and prepared it from natural GM1 by chemo-enzymatic processes summarized in Figure 4a. The natural GM1 was a 1:1 mixture of two homologues having different side chains (R = $C_{13}H_{27}$ and $C_{15}H_{31}$). The *N*-acyl group in the natural GM1 was removed with sphingolipid ceramide *N*-deacylase[41,42] to yield the *lyso*-GM1 homologues (R = $C_{13}H_{27}$ + $C_{15}H_{31}$) carrying amino groups. The two homologues of *lyso*-GM1 could be readily separated with an ODS HPLC column. In this study, the GM1 homologue with a shorter alkyl chain (R = $C_{13}H_{27}$) was used. This amino group was then reacted with NHS ester of lipoic acid to produce the target compound **3**, which was immobilized on the Au nanoparticles (Figure 4b).

After the GM1 derivative **3** was immobilized on the Au surface for CTX detection, an excess amount of lipoic acid was added to the GM1-coated chip surface to block nonspecific binding of BSA on open areas of the Au nanoparticles (Figure 4c). Alkane thiol is often used as a blocking agent;[43] however, we used the more polar lipoic acid to eliminate a nonspecific hydrophobic interaction with the ceramide alkane group. Figure 4d shows that the blocking process was very effective for suppressing nonspecific binding of BSA onto the GM1 chips and also for improving the detection sensitivity of CTX. Prior to the blocking process, BSA was able to access hydrophobic environments through spaces in the GM1 cluster. Many proteins may be blocked in this way, and the blocking process may change the spatial arrangement of the GM1 clusters to some extent, bringing about higher sensitivity to CTX.

Figure 5a shows that the detection sensitivity in the GM1 chips was dependent on the size of the Au nanoparticles, with a maximum sensitivity of 20 ng/mL CTX at 40 nm (Figure 5b). Reference proteins such as peanut (*Arachis hypogaea*), wheat germ (*Triticum vulgaris*), *Sambucus nigra*, horse gram (*Dolichos biflorus*), BSA, and ricin showed no response at concentrations as high as 300 ng/mL (Figure 5b), demonstrating the high selectivity of the LSPR system using the optimal GM1 chip.

Figure 6 shows that LSPR responses are linear as a function of toxin concentrations up to 100 ng/mL. On the basis of theses curves, the detection limit was determined and tabulated in Table 1.

Nath and Chilkoti reported that LSPR sensitivity is dependent on Au nanoparticle size and can be optimized for each interacting molecule.[34−36] The response is thought to be dependent not only on the bulk refractive index associated with the size of Au particles but also on the local refractive index associated with the size of the immobilized probe molecules and the target molecules bound on the probes. Table 1 summarizes the optimal conditions for each of the biological toxins. The LSPR sensitivity is expected to increase with Au nanoparticle size when the bulk refractive index is considered.[32−37] However, that was not observed here, since the largest (100-nm) particles were not effective for any toxin. Therefore, it appears that the local refractive index is more important. In our analysis, the net volumes of the three toxins are all in the range of 10 × 10 × 10 nm. Therefore, the differences in the optimal Au nanoparticle sizes must arise largely from differences in the size, polarity, and geometry of the carbohydrate ligands immobilized on the nanoparticles. This also indicates that the density of the sugar ligands may affect the local refractive index; thus, the optimal Au nanoparticle size may vary with different immobilization reaction conditions.

dx.doi.org/10.1021/am4002937 | ACS Appl. Mater. Interfaces 2013, 5, 4173−4180

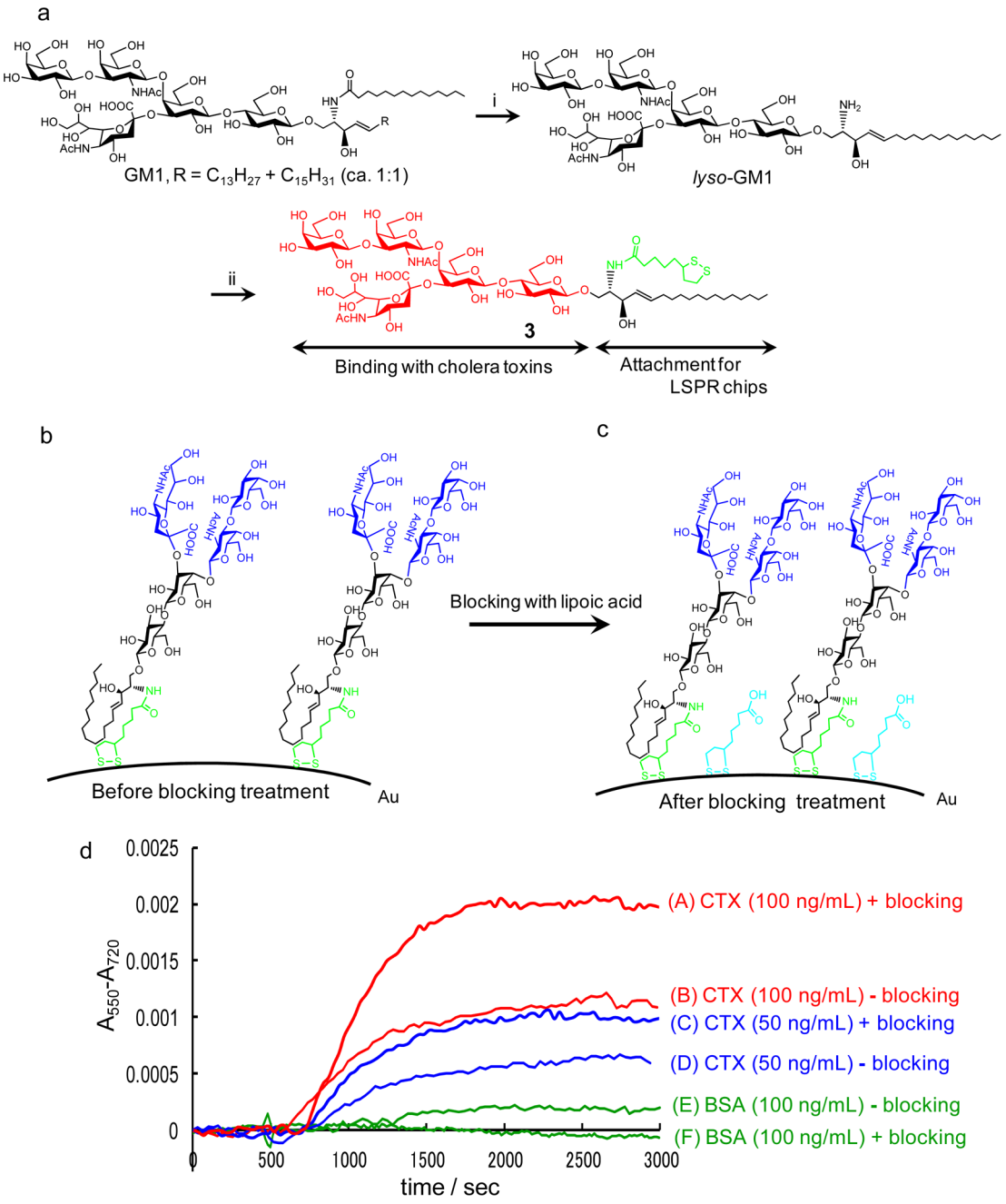

Figure 4. (a) Preparation of GM1 pentasaccharide **3**. Conditions for the synthesis of **3**: (i) Sphingolipid ceramide *N*-deacylase in a 50 mM AcONa-AcOH buffer (pH 6.0) containing 1% sodium taurodeoxycholate. (ii) NHS ester of lipoic acid. (b, c) GM1-chips for the LSPR detection of CTX. (d) Results of LSPR detection of CTX before and after blocking treatment of the Au-surface with lipoic acid. Au-size: 40 nm. Samples were injected at 500 s.

CONCLUSIONS

We have demonstrated LSPR detection systems for biological toxins that utilize glyco-chips. We have presented a general process for the immobilization of natural glycosyl ceramides on Au nanoparticles to make the glyco-chips. It was found that optimizing the Au nanoparticle diameter size is critical to each LSPR system. For the detection of cholera toxin by using GM1 chips, a lipoic acid blocking process on the Au surface was required to prevent nonspecific protein detection. This step was not required for the ricin and Stx-1 chips and most likely occurs because the GM1 chips have more available space between the GM1 molecules, allowing access to the hydrophobic ceramide moiety. Detection sensitivity was in a range between 10−30 ng/mL and was nearly equal for the three toxins. For every case, the LSPR detection was completed within 20 min and was highly specific to the target toxin. The three toxins examined in this study have different molecular sizes and subunit structures, and they recognize different oligosaccharides. Therefore, optimization processes for each of the glyco-chips is required to gain higher sensitivity and selectivity.

The immunological approach of enzyme-linked immuno sorbent assays,[22,44−49] the genetic approach of polymerase chain reaction,[50−53] and the spectroscopic approaches of surface plasmon resonance, mass spectroscopy, and other analytical instruments[54−58] have already been proposed for

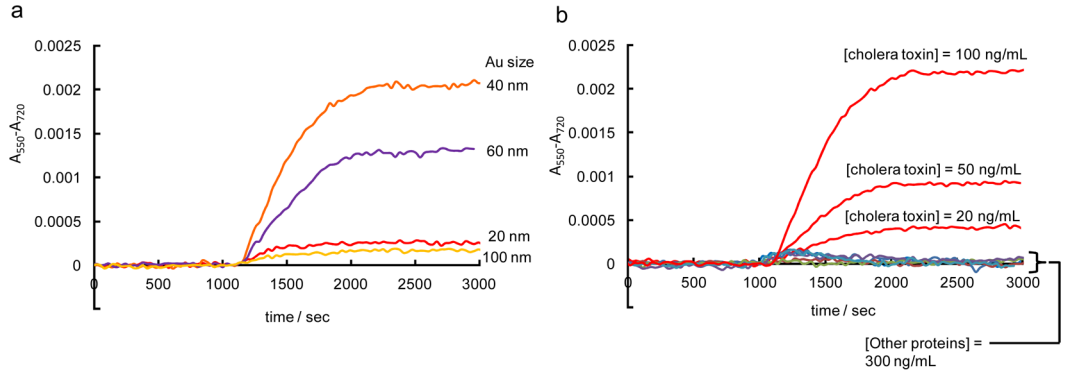

Figure 5. LSPR detection of cholera toxin using GM1-functionalized chips after blocking treatment. (a) Effect of Au nanoparticle diameter size. [cholera toxin] = 100 ng/mL. (b) LSPR response to cholera toxin at different concentrations and also to other reference proteins at 300 ng/mL. Reference proteins: peanut lectin, *Triticum vulgaris* lectin from wheat germ, *Sambucus nigra*, *Dolichos biflorus* lectin from horse, BSA, and ricin. Au-size: 40 nm. All samples were injected at 1000 s. A blocking process was performed with lipoic acid to eliminate nonselective binding of other proteins and also to achieve a specific binding interaction with CTX.

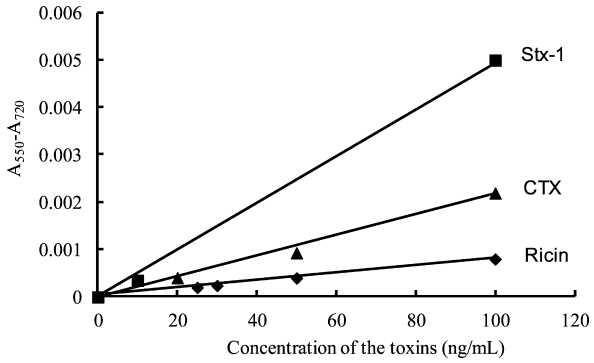

Figure 6. LSPR responses (A_{550}–A_{720}) as a function of toxin concentrations.

Table 1. Summary of LSPR Detection Systems

	glyco-chips			
toxins	sugars	Au particles[a]	blocking process[b]	limit of detection (ng/mL)
ricin	lactoside **1**	20 nm	not required	30
Shiga toxin (Stx-1)	Gb_3 **2**	40 nm	not required	10
cholera toxin (CTX)	GM1 **3**	40 nm	required	20

[a]Diameter of optimum Au nanoparticles. [b]Blocking process by lipoic acid.

biological toxin analysis. Because of its sensitivity, a LSPR system based on glyco-nanotechnology is competitive with these other techniques and has the added advantage of being portable and for providing simple and rapid analysis in contaminated areas.

AUTHOR INFORMATION

Corresponding Author

*E-mail: h.uzawa@aist.go.jp. Tel: +81-29-861-4778.

Notes

The authors declare no competing financial interest.

ACKNOWLEDGMENTS

We thank Dr. Koji Ohga (AIST) for his primary contribution and Prof. Norihiko Minoura (Tokyo University of Technology) and Drs. Toshio Shinbo (AIST), Yukiko Shinozaki (AIST), and Daisuke Nishida (AIST) for their help at the exploratory stage of this work. This work was financially supported by "a R&D Program for Implementation of Anti-Crime and Anti-Terrorism Technologies for a Safe and Secure Society", Funds for Integrated Promotion of Social System Reform and Research and Development of the Ministry of Education, Culture, Sports, Science and Technology (MEXT) of Japan, and a Grant-in-Aid for Scientific Research from MEXT.

REFERENCES

(1) (a) Mayer, K. M.; Hafner, J. H. *Chem. Rev.* **2011**, *111*, 3828–3857. (b) Saha, K.; Agasti, S. S.; Kim, C.; Li, X.; Rotello, V. M. *Chem. Rev.* **2012**, *112*, 2739–2779.
(2) Sepúlveda, B.; Angelomé, P. C.; Lechuga, L. M.; Liz-Marzán, L. M. *Nano Today* **2009**, *4*, 244–251.
(3) Endo, T.; Kerman, K.; Nagatani, N.; Hiep, H. M.; Kim, D.-K.; Yonezawa, Y.; Nakano, K.; Tamiya, E. *Anal. Chem.* **2006**, *78*, 6465–6475.
(4) Hiep, H. M.; Nakayama, T.; Saito, M.; Yamamura, S.; Takamura, Y.; Tamiya, E. *Jpn. J. Appl. Phys.* **2008**, *47*, 1337–1341.
(5) Sanvicens, N.; Pastells, C.; Pascual, N.; Marco, M.-P. *Trends Anal. Chem.* **2009**, *28*, 1243–1252.
(6) Haes, A. J.; Hall, W. P.; Chang, L.; Klein, W. L.; Duyne, R. P. V. *Nano Lett.* **2004**, *4*, 1029–1034.
(7) Hall, W. P.; Ngatia, S. N.; Van Duyne, R. P. *J. Phys. Chem. C* **2011**, *115*, 1410–1414.
(8) Mayer, K. M.; Lee, S.; Liao, H.; Rostro, B. C.; Fuentes, A.; Scully, P. T.; Nehl, C. L.; Hafner, J. H. *ACS Nano* **2008**, *2*, 687–692.
(9) Wang, X.; Li, Y.; Wang, H.; Fu, Q.; Peng, J.; Wang, Y.; Du, J.; Zhou, Y.; Zhan, L. *Biosens. Bioelectron.* **2010**, *26*, 404–410.
(10) Huang, H.; He, C.; Zeng, Y.; Xia, X.; Yu, X.; Yi, P.; Chen, Z. *Biosens. Bioelectron.* **2009**, *24*, 2255–2259.
(11) Yoo, S. Y.; Kim, D.-K.; Park, T. J.; Kim, E. K.; Tamiya, E.; Lee, S. Y. *Anal. Chem.* **2010**, *82*, 1349–1357.
(12) Bi, N.; Sun, Y.; Zhang, H.; Song, D.; Wang, L.; Wang, J.; Tian, Y. *Colloids Surf., B* **2010**, *81*, 249–254.
(13) Yonzon, C. R.; Jeoung, E.; Zou, S.; Schatz, G. C.; Mrksich, M.; Van Duyne, R. P. *J. Am. Chem. Soc.* **2004**, *126*, 12669–12676.
(14) Vikesland, P. J.; Wigginton, K. R. *Environ. Sci. Technol.* **2010**, *44*, 3656–3669.
(15) Varki, A., Cummings, R., Esko, J., Freeze, H., Hart, G., Marth, J., Eds. *Essentials of glycobiology*; Cold Spring Harbor Laboratory: Spring Harbor, NY, 1999; pp 429–440.
(16) Uzawa, H.; Ohga, K.; Shinozaki, Y.; Ohsawa, I.; Nagatsuka, T.; Seto, Y.; Nishida, Y. *Biosens. Bioelectron.* **2008**, *24*, 929–933.

(17) Uzawa, H.; Kamiya, S.; Minoura, N.; Dohi, H.; Nishida, Y.; Taguchi, K.; Yokoyama, S.; Mori, H.; Shimizu, T.; Kobayashi, K. *Biomacromolecules* **2002**, *3*, 411−414.
(18) Uzawa, H.; Ito, H.; Neri, P.; Mori, H.; Nishida, Y. *ChemBioChem* **2007**, *8*, 2117−2124.
(19) Johnston, D.; Hulse, C. *The New York Times*, February 2, 2004. http://www.nytimes.com/2004/02/04/us/ricin-capitol-hill-overview-finding-deadly-poison-office-disrupts-senate.html?pagewanted)1.
(20) http://emergency.cdc.gov/agent/agentlist-category.asp. (Accessed August, 2012).
(21) Kaper, J. B., O'Brien, A. D., Eds. *Escherichia coli O157:H7 and Other Shiga Toxin-Producing E. coli Strains*; ASM Press: Washington, DC, 1998.
(22) Pilch, R. F., Zilinskas, R. A., Eds. *Encyclopedia of Bioterrorism Defense*; John Wiley & Sons: Hoboken, NJ, 2005 and references cited therein.
(23) Montfort, W.; Villafranca, J. E.; Monzingo, A. F.; Ernst, S. R.; Katzin, B.; Rutenber, E.; Xuong, N. H.; Hamlin, R.; Robertus, J. D. *J. Biol. Chem.* **1987**, *262*, 5398−5403.
(24) Baenziger, J. U.; Fiete, D. *J. Biol. Chem.* **1979**, *254*, 9795−9799.
(25) Wu, J. H.; Singh, T.; Herp, A.; Wu, A. M. *Biochimie* **2006**, *88*, 201−217.
(26) Endo, Y.; Mitsui, K.; Motizuki, M.; Tsurugi, K. *J. Biol. Chem.* **1987**, *262*, 5908−5912.
(27) Sphyris, N.; Lord, J. M.; Wales, R.; Roberts, L. M. *J. Biol. Chem.* **1995**, *270*, 20292−20297.
(28) Merritt, E. A.; Hol, W. G. J. *Curr. Opin. Struct. Biol.* **1995**, *5*, 165−171.
(29) Ling, H.; Boodhoo, A.; Hazes, B.; Cummings, M. D.; Armstrong, G. D.; Brunton, J. L.; Read, R. J. *Biochemistry* **1998**, *37*, 1777−1788.
(30) Nutikka, A.; Lingwood, C. *Glycoconjugate J.* **2003**, *20*, 33−38.
(31) Lingwood, C. A. *Trends Glycosci. Glycotechnol.* **2000**, *12*, 7−16.
(32) Khlebtsov, N. G.; Dykman, L. A.; Bogatyrev, V. A.; Khlebtsov, B. N. *Colloid J.* **2003**, *65*, 508−517.
(33) Khlebtsov, N. G. *J. Quant. Spectrosc. Radiat. Transfer* **2004**, *89*, 143−153.
(34) Nath, N.; Chilkoti, A. *Anal. Chem.* **2004**, *76*, 5370−5378.
(35) Nath, N.; Chilkoti, A. *Anal. Chem.* **2002**, *74*, 504−509.
(36) Nath, N.; Chilkoti, A. *J. Fluoresc.* **2004**, *14*, 377−389.
(37) Frederix, F.; Friedt, J.-M.; Choi, K.-H.; Laureyn, W.; Campitelli, A.; Mondelaers, D.; Maes, G.; Borghs, G. *Anal. Chem.* **2003**, *75*, 6894−6900.
(38) Nagatsuka, T.; Uzawa, H.; Ohsawa, I.; Seto, Y.; Nishida, Y. *ACS Appl. Mater. Interfaces* **2010**, *2*, 1081−1085.
(39) Sack, D. A.; Sack, R. B.; Nair, G. B.; Siddique, A. K. *Lancet* **2004**, *363*, 223−233.
(40) (a) Moss, J.; Vaughan, M. *Annu. Rev. Biochem.* **1979**, *48*, 581−600. (b) Merritt, E. A.; Sarfaty, S.; van den Akker, F.; L'Hoir, C.; Martial, J. A.; Hol, W. G. J. *Protein Sci.* **1994**, *3*, 166−175.
(41) Kurita, T.; Izu, H.; Sano, M.; Ito, M.; Kato, I. *J. Lipid Res.* **2000**, *41*, 846−851.
(42) Larsson, E. A.; Olsson, U.; Whitmore, C. D.; Martins, R.; Tettamanti, G.; Schnaar, R. L.; Dovichi, N. J.; Palcic, M. M.; Hindsgaul, O. *Carbohydr. Res.* **2007**, *342*, 482−489.
(43) Aqua, T.; Naaman, R.; Daube, S. S. *Langmuir* **2003**, *19*, 10573−10580.
(44) Walt, D. R.; Franz, D. R. *Anal. Chem.* **2000**, *72*, 738A−746A.
(45) Taitt, C. R.; Anderson, G. P.; Lingerfelt, B. M.; Feldstein, M. J.; Ligler, F. S. *Anal. Chem.* **2002**, *74*, 6114−6120.
(46) Rowe-Taitt, C. A.; Cras, J. J.; Patterson, C. H.; Golden, J. P.; Ligler, F. S. *Anal. Biochem.* **2000**, *281*, 123−133.
(47) Leith, A. G.; Griffiths, G. D.; Green, M. A. *J. Forensic Sci. Soc.* **1998**, *28*, 227−236.
(48) Weeratna, R. D.; Doyle, M. P. *Appl. Environ. Microbiol.* **1991**, *57*, 2951−2955.
(49) Acheson, D. W. K.; Jacewicz, M.; Kane, A. V.; Donohue-Rolfe, A.; Keusch, G. T. *Microb. Pathog.* **1993**, *14*, 57−66.
(50) He, X.; Brandon, D. L.; Chen, G. Q.; McKeon, T. A.; Carter, J. M. *J. Agric. Food Chem.* **2007**, *55*, 545−550.
(51) Lubelli, C.; Chatgilialoglu, A.; Bolognesi, A.; Strocchi, P.; Colombatti, M.; Stirpe, F. *Anal. Biochem.* **2006**, *355*, 102−109.
(52) He, X.; Carter, J. M.; Brandon, D. L.; Cheng, L. W.; McKeon, T. A. *J. Agric. Food Chem.* **2007**, *55*, 6897−6902.
(53) Tsen, H.-Y.; Jian, L.-Z. *J. Appl. Microbiol.* **1998**, *84*, 585−592.
(54) Kalb, S. R.; Barr, J. R. *Anal. Chem.* **2009**, *81*, 2037−2042.
(55) Chen, G.; Ning, X.; Park, B.; Boons, G.-J.; Xu, B. *Langmuir* **2009**, *25*, 2860−2864.
(56) Stine, R.; Pishko, M. V.; Schengrund, C.-L. *Langmuir* **2004**, *20*, 6501−6506.
(57) Gustafson, I. *Colloids Surf., B* **2003**, *30*, 13−24.
(58) Puu, G. *Anal. Chem.* **2001**, *73*, 72−79.